EMC2®

EMC2 Inertial-Electrostatic Fusion (IEF) Development:

Final Successful Tests of WB-6; October/November 2005

Robert W. Bussard and R. Michael Wray

EMC2-0806-04
rev. 0107

EMC2

ENERGY/MATTER CONVERSION CORPORATION
680 Garcia St., Santa Fe, NM 87505. 505-988-8948
emc2qed@comcast.net

Introduction

WB-6 was the last in a series of fusion experiments run at EMC2. Like its predecessors, WB-1, WB-2, WB-3 and WB-4, it was an arrangement of circular magnetic coils, set up as a truncated cube. It utilized six circular coils of approximately 3 cm cross-sectional diameter, with 200 turns of copper wire conductor in each coil, all connected in series, and each coil was approximately 30 cm in diameter. The coil containers were toroidal, in order to approximate conformal surfaces with the geometry of the B fields produced by the windings they contained. Figures 1,2, and 3 show the general layout of this device, and a picture of its coils in one stage of assembly.

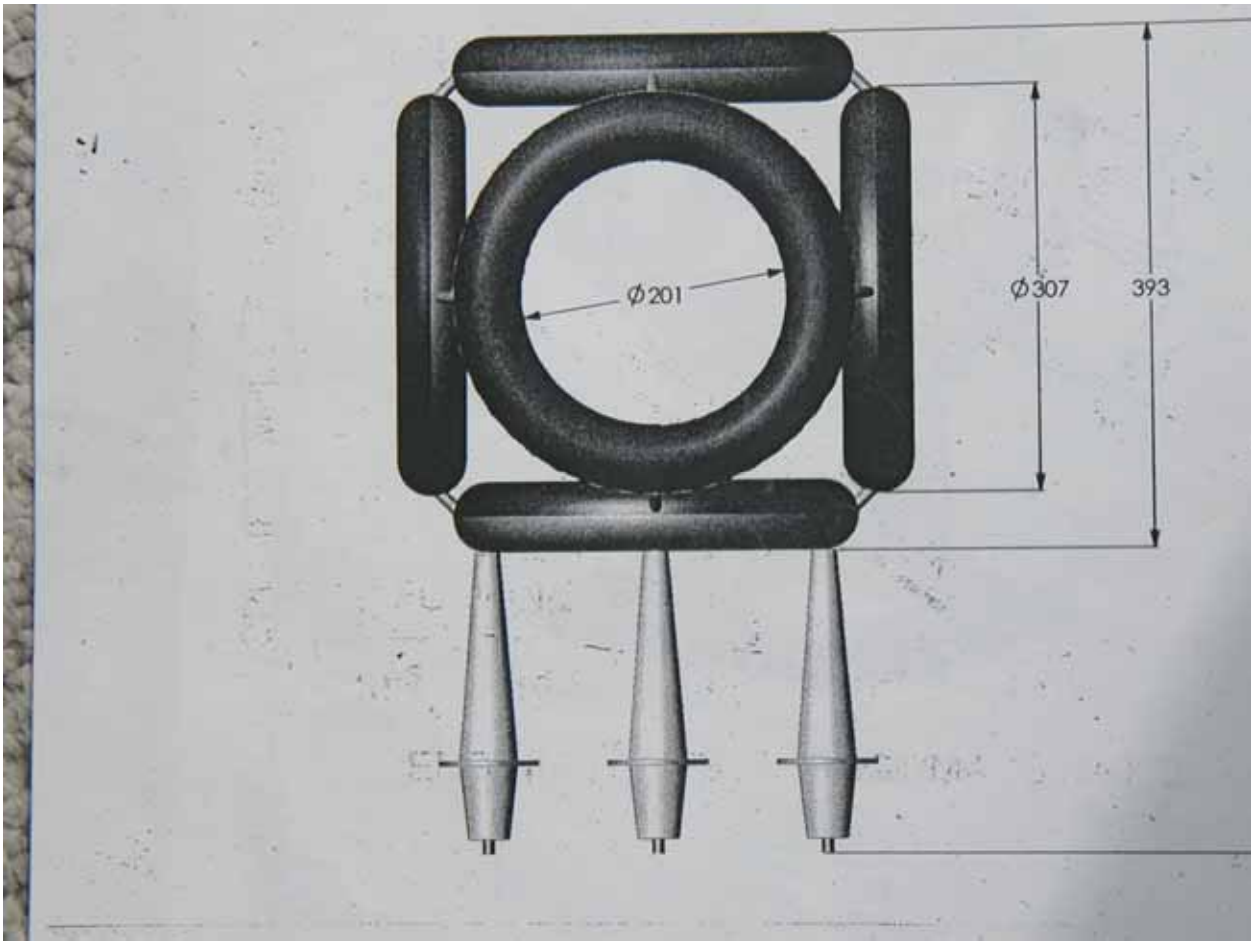

Figure 1. WB-6 layout, showing spacing between coils at "corners." Note that the tubular interconnects are located outside the mid-plane of the magnetic field of the coils.

Figure 2. WB-6 coils, showing 200-turn windings and interconnects between coil containers

Energetic electrons were injected into this device along cusp axes, and trapped by the polyhedral configuration of the magnetic fields. Electrons so injected were free to move along field lines, and thus to circulate from the interior of the machine out through the cusps, and thence back into the machine again. This recirculating configuration was called a Magnetic Grid machine, or MaGrid machine.

Electron Trapping

Its ability to trap electrons inside the device is measured by an overall trapping factor, called Gmj, which is the ratio of the electron lifetime in the machine environment with B fields turned on

Figure 3. WB-6 as finally assembled before testing, October 2006. Tapered ceramic posts contain the main power feedthrough conductors to the wound coil system.

to that with no B fields. This overall e- current trapping factor is composed of two terms; one due to internal trapping by diamagnetic electron confinement leading to cusp confinement, and one due to electron trapping/flow through coil corner positions, which act somewhat like line cusps.

The first of these represents the effect of B field expansion under electron pressure, and is called the Wiffle-Ball factor (derived from the geometry of the child's perforated toy ball, called a Wiffle Ball) Gwb. This effect acts to reduce cusp/axis loss area as the B field is expanded to its limit at the beta=one condition (i.e. when electron kinetic pressure equals magnetic pressure) and thus to limit the effective size of the loss holes on the cusp axes, as seen by electrons as they repetitively traverse the interior of the machine. For a truncated cube geometry (used in all machines tested to date) this factor is Gwb = (BR)^2/110Eo, where B is the magnetic field strength (in G) on-axis of the main faces, R is the radius of the device (in cm) from its center to the midplane of the field coils, and Eo is the depth of the electric potential well (in eV) resulting from the injection of the energetic electrons that drive the device. Typically the well depth is about 0.7-0.9 of the electron injection energy (Ei), depending on the exact geometry of the device and of the injection system. In WB-6 well depth was about 0.8 of injection energy.

The second of these is the coil corner flow trapping, in which the B fields at and along the corner positions are not simple single cusps but, rather, are semi-line-cusp as the coils bend around each corner. The trapping factor here is just that due to electron reflection from the effective line cusp over the (small) area of the corner "touching" points. This factor is given by the ratio of free flow current (without B field) to that with B field, and is called Glc. Analysis of the reflection of electrons from line cusps shows that this is approximately equal to the square root of the Mirror Reflection factor from single axial point cusps, Gmr, thus Glc = SQRT(Gmr).

Gmr is simply the ratio of the maximum B field strength at the center of the point or line cusp, Bo, to that field at which electrons are adiabatically captured (Bad) as they approach the cusp. The adiabatic capture radius (position) is given by the condition that the fractional change in the gyro radius of the electrons be less than the fractional change in B field over any given distance; (rgyro)[dLN(B)/dr] < 2/3. For the polyhedral B fields of interest here [$B = Bo(r/R)^m$] this is found to be

Gmr = Bo/Bad = [2BoR/9mSQRT(Ei)]^(3/4)

As an example,, for Ei = 1E4 eV, Bo = 1E4 G. and R = 30 cm, with m = 3 (truncated cube at very small beta) this gives Gmr = 57.5, and hence Glc = 7.6

It is immediately obvious that flow through the corner line cusps will be much greater, per unit area, than flow through the WiffleBall point cusps of these machines. These two circulation flow channels lead to the overall trapping factor Gmj as a parallel channel sum of each of them, weighted by the fractional area of the machine envelope occupied by each channel effect. Taking

fwb and flc as the fractional areas of point cusp and line cusp effects (note that fwb + flc = 1), and summing for parallel channel flow, gives the overall trapping factor as

$$(1/Gmj) = (fwb/Gwb) + (flc/Glc)$$

If all electron flow were to be governed by the line cusp/corner effects, it would be virtually impossible to maintain high electron densities inside the machine while keeping densities outside low enough to avoid Paschen arcing outside. Fortunately this is somewhat under the control of the machine design, which can be made so that the fractional line cusp area is quite small;. The line cusp flow effect can be kept from dominance only if the fractional area involved is less than the ratio of Glc to Gwb in the system. If the two effects are equal the overall trapping factor will be reduced from the pure WB effect by a factor of two. This is seen by writing the overall trapping factor as

$$Gmj = Gwb/[fwb + flc(Gwb/Glc)]$$

As previously discussed, Gmj is the ratio of electron lifetime in the machine environment with fields turned on to that with no fields. The importance of this is that this is equal to the ratio of electron density inside the machine to that found outside; the purpose of such trapping is to allow the attainment of high density of electrons within the field configuration – to allow consequent attainment of high density of ions also therein - while still maintaining low density outside – to avoid external Paschen arcing. Without arcing, the trapped electrons inside the system form a quasi-stable cloud in the center of the device, making a negative electrostatic potential "well", which then traps positive ions within its electric structure, but only up to the density of electrons also trapped within..

Arcing

Arcing, either inside or outside the machine system, is the most damaging electron loss mechanism. To control arc formation it is necessary to avoid all sharp corners (which enhance local E fields) and unshielded (by B fields) metal surfaces in the entire system. Figure 4 shows the Paschen curve for arc formation between parallel plane plates in H2 and other gases. Note that the criterion for arc formation is the product of spacing (d) and background gas pressure (p).

In the systems of concern here, the effective spacing is that distance over which an electron will travel before it hits the opposing wall or surface. For high Gmj factors this means that the internal path length is the actual physical spacing multiplied by the Gmj factor. The same is true for electrons external to the system, if they are recirculated by the configuration of B field trapping. These curves are shifted markedly to lower breakdown voltages at the low end of the (pd) product parameter, if sharp corners and edges mark the surfaces over which arcing may occur.

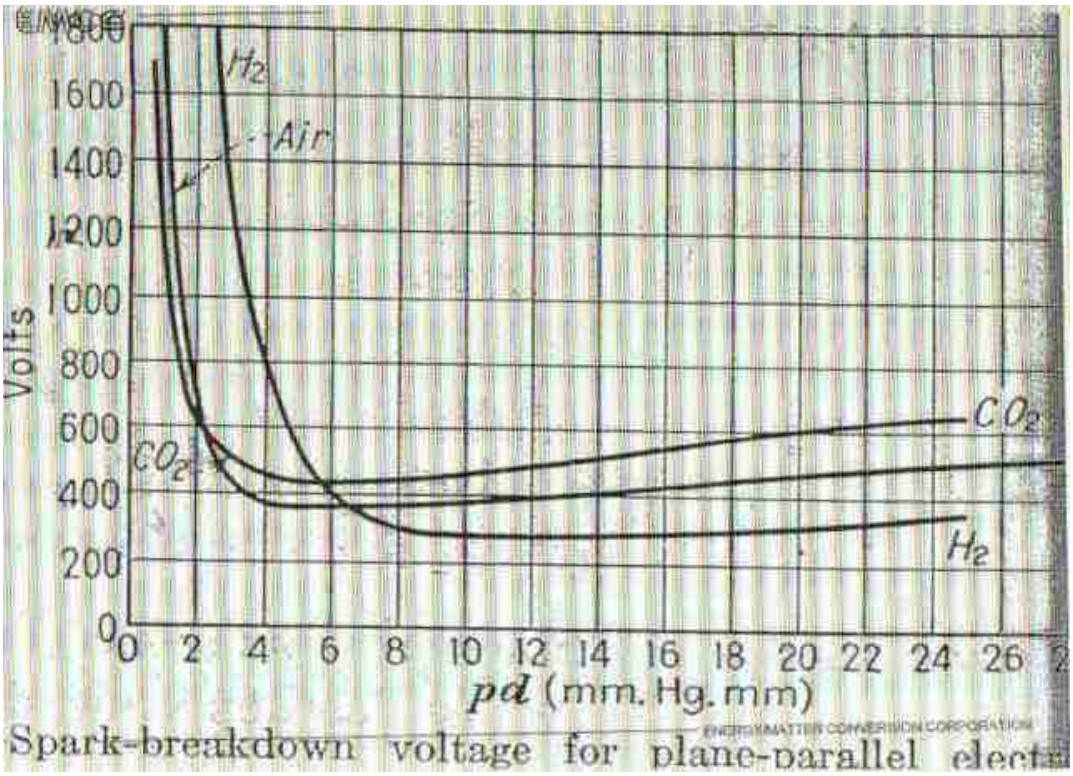

Figure 4. Paschen curves for arc breakdown; plane parallel electrodes only. Edges and sharp projections and corners may enhance this – leading to breakdown at smaller (pd) values by as much as a reduction of 10x or more.

Arcing can take place *inside* the system whenever sufficient deviation from local B field insulation is driven by "pinch effect" currents to the otherwise shielded metal surfaces. The arc pinch B field is given as Bp = 0.2Ip/rp, where Ip is the pinch current and rp is its radius (gaussian units), and Ip = (pi)(rp)^2(jp), where jp is the pinch current density (A/cm2), this becomes Bp = 0.2pi(jp)(rp) for B in Gauss. Now the condition for arc formation is when the pinch field significantly disturbs the shielding main B field Bo, thus when |Bo-Bp| << Bo. This yields the constraint that Bp/Bo << 1, or that Bo >> 0.2pi(jp)(rp).

From MHD stability theory (and copious experiments since 1955) it has been found that pinch discharges are inherently unstable if current densities and radii are above some defined levels in any system. The condition is approximately given by rb^2 > 3E9[SQRT(Ee)]/ne; this yields rb > 0.2 cm for typical conditions of interest. Thus, it is possible to suppress such effects by avoiding all sharp corners and electric field focus points in the design and construction of the interior of the device, so as to prevent the attainment of high current densities over very small areas in arc formation.

Electron Losses and Machine Impedance.

This can also be viewed is a matter of controlling the overall circuit impedance Z of the machine test system as it runs. This impedance is simply the ratio of electron drive injection energy to the electron current e-losses to the machine (not to the walls and tanks) in machine operation. This, in turn, is dominated by the three factors in e-loss phenomena:

1. direct MG transport through the B-shielded surfaces, Img,
2. e-losses to poorly shielded or unshielded metal surfaces, Iunsh, and
3. losses due to local arcing, Iarc.

Thus Z = Ee/Iej, where Iej = Img + Iunsh + Iarc, is the sum of these three e-loss currents.

The third of these, arc currents, have been discussed in a preceding section. In general, these small scale, small diameter high-current arcs Iarc are not easily quantified, as they depend on details of the configuration of the surfaces which may be involved in the arcing process. As previously noted, these can be avoided only by careful design of all surfaces so that there are NO edges or sharp corners, and so that all surfaces are either conformal to insulating B fields or electrostatically insulated by applied potentials. If these design conditions are met, it is not possible for arcs to form. Arcing from the emitters to the machine will always destroy the drive potential, and can not be tolerated, thus design for arc suppression is essential. And, as a practical matter, design for arc suppression must also be made for all aspects of the test system (e.g. tank wall to feedthroughs, etc) as arcing anywhere in the high voltage drive system will also shut the system down, sometimes with damage to the device or its supporting components.. This is not difficult, but does require close attention to the details of the entire mechanical/electrical system used for testing.

.

In an arc-suppressed machine, only the first two of these current loss effects will occur. Studies, experiments and analyses made over the R&D program period have given a good understanding of the Img MG loss current effects, and shown the form of the equation describing these. Losses to poorly-shielded surfaces, Iunsh are analogous to (but not the same as) the line cusp flow loss effects previously discussed. Both of these are discussed further in a following section.

The key to successful operation of this (or any other Polywell) machine is to minimize electron *losses,* which are the dominant power losses in the device. To this end, WB-6 was designed to incorporate the discovery made in testing of the closed box machine (i.e. a device whose coils were outside a closed vacuum box, and in which electrons could not recirculate), WB-5, during Spring and Summer 2005. This device is pictured in Figure 5, which shows the unshielded (by B fields) edges and corners of the closed-box structure.

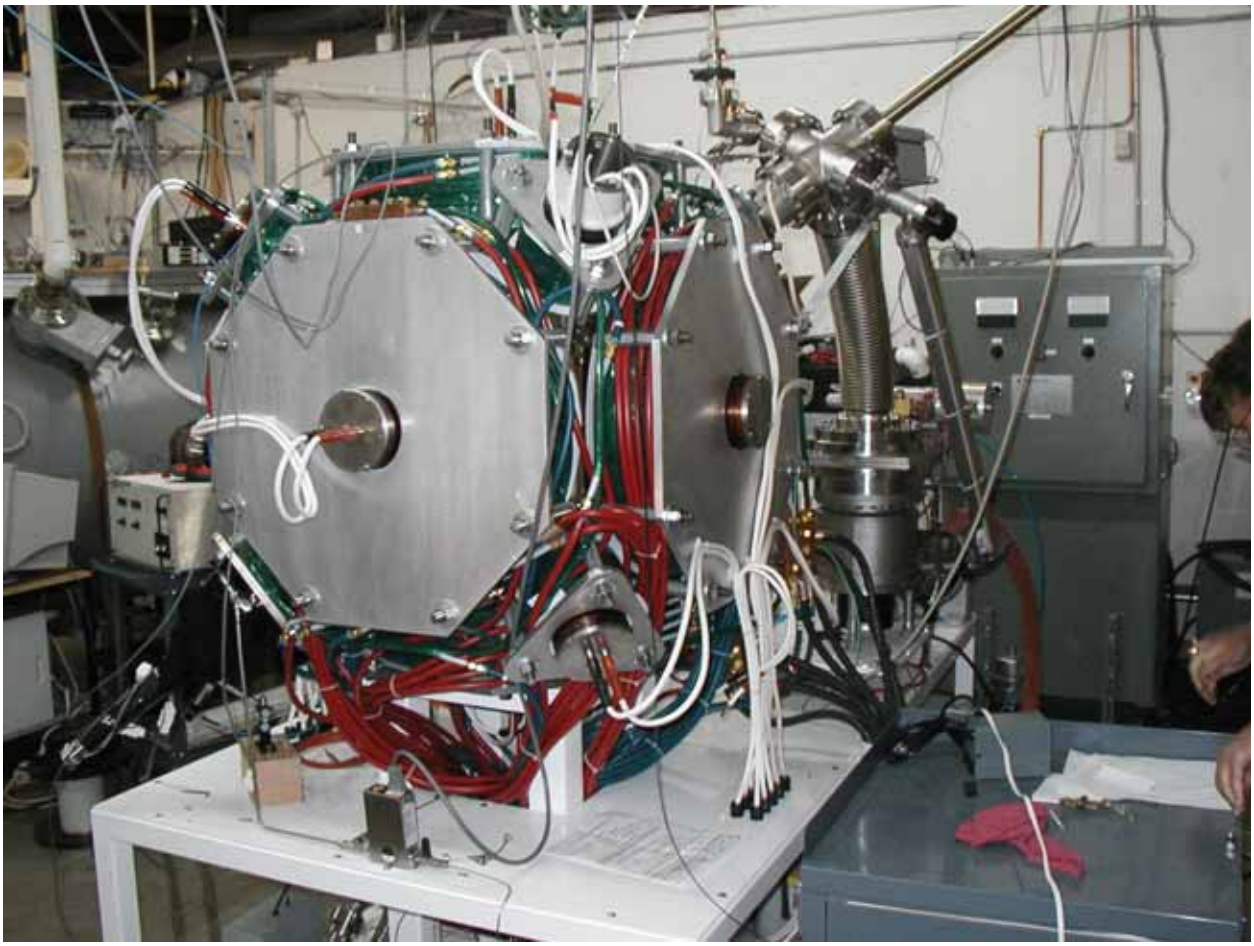

Figure 5. WB-5; note cusp axis end plates, edges and corners not shielded by B field coils

This testing showed conclusively that electron losses can not be avoided due to B field penetrations of the box walls at the seams and corners of the structure, which result in direct impact paths for electrons which find themselves trapped in motion on these wall-intersecting B fields. There does not appear to be any (practical engineering) way to cover ALL of such a box surface with protective B fields. Electron losses due to this effect would add another term to Gmj; one to account for losses to a fractional area over which B fields intersected the structure. Simple analysis shows that the fractional area of such intercept that can be tolerated within the requirement for net fusion power is less than 1E-4 to 1E-5, well below the values allowed for the line cusp flow channel effect.
.

Thus WB-6 was designed and built with coil container shells that were conformal to the B field shapes produced by the coils so contained, thus eliminating the electron-intercepting corners of the rectangular cross-section coil containers used in all prior machines (except MPG-1,2). It was

also designed with a significant spacing between coils at their otherwise-touching corners, so as to eliminate any direct B field intersection with container surfaces at these positions, and thus to prevent any direct electron transport along field lines into the metal. The spacing was chosen to provide electron gyro radii at the line cusp center plane of about 1/3 the spacing between coils. Larger spacing would reduce wall impact probabilities but only at the price of increased line cusp channel flow, with larger fractional line cusp area contribution, and thus lower values of Gmj. Detailed design here will lead to optimization of the spacing to maximize overall performance. Insufficient time was available to undertake such detailed design analyses for WB-6, and the dimensions chosen were based on general considerations of gyro radius effects in the flow channel.

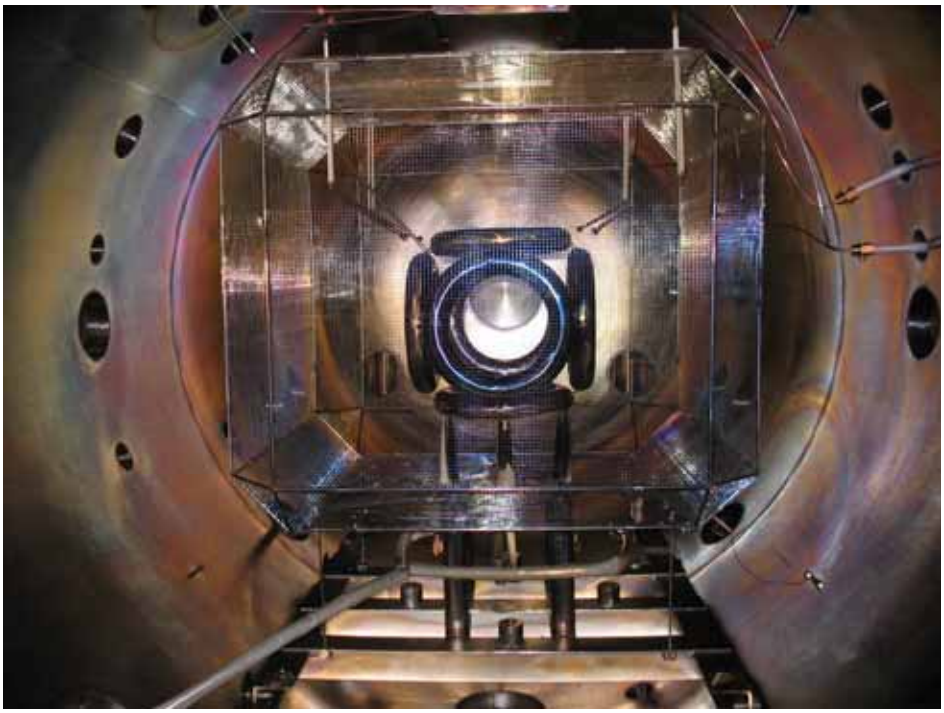

Figure 6 WB-5 in test tank, inside grounded Faraday cage; emitters on triangular corners

With these design features, the WB-6 device was hastily constructed in August/September 2005, and put into the large vacuum, system, inside a grounded potential cage, for testing. Figure 6 shows this arrangement in the EMC2 labs in San Diego. The machine was held at high positive potential, to act as an electron attractor for emission from the emitters which were placed on four corners of the configuration (on triangular corners of the truncated cube, approximated using circular coils, as in previous WB/MG machines).

The emitters (which were each simply an array of tungsten headlight filaments) were also held at ground potential; thus the only element in the machine system not at ground was the WB-6

device, itself, into which electrons were injected from the emitters spaced a short distance from the device, and on-axis of the corner cusps. The emitter standoff distance was kept approximately equal to the mean radius of the cusp face through which they were injected. This minimized electrostatic "droop" in the potential well at these corners, yet gave sufficient potential field gradient to provide good extraction from the filaments.

Short-Pulse Machine Operation; WB-6

The electrons thus injected at the high energy of the device positive potential, then ionized the fusion fuel deuterium (D2) gas that was next injected, into the interior of the system, through a small tube leading directly into the edge of a cusp face. This was done to attempt to keep the neutral gas density inside the machine higher than that outside, during its very short time of initial operation, while the external gas pressure – hopefully - remained low (to prevent arcing) for a short period until the outflow of injected gas filled the main vacuum tank. The residence time of neutral gas atoms in the machine is about 0.3 msec, thus gas not ionized in this time will escape into the space surrounding the device, between the device and the Faraday cage (screen) external to the machine, which provides a spatially congruent electric potential (at ground) for the test.

Energetic electrons injected into this neutral gas buildup ionizes some of this gas, with an ionization time of about 0.3-0.5 msec, producing ions of D. These then begin to fall into the potential well – as it forms - along its electrostatic field gradients. Ionization was, in the first moment of injection of electrons, done solely by the fast injected electrons. However, the electron/ion density thus produced (initially only by fast electron ionization) was too low to satisfy the beta=one condition, and many of the neutral atoms escaped without ionization.

However, as this initial ionization proceeded, the low energy electrons (at ca. 100 eV) produced by such ionization of each neutral atom of D, then collided with other D atoms, and ionized them in an exponentially-growing cascade. This is especially important to note, because the cross-section for ionization by low energy electrons is much larger than by fast electrons (e.g. at the injection energy of ca. 12-12.5 keV). At low energy the cross-section is approximately (sigmaizn) = 1E-16 cm2, while at the high drive energy of injection the cross section is of order 0.3-1E-17 cm2. The e-folding time for this cascade is about 2 usec (microsec). Since the stable density attainable by the injected electrons is only about 1E9/cm3, while the neutral gas density is in the range of 2-5E12/cm3, the cascade must increase the electron density by roughly 4000x to reach nearly total ionization. This is only about 9 e-foldings, thus the entire secondary low-energy ionization process requires only about 20 usec to complete.

As this process proceeded, the increasing and large density of initially-low-energy (i.e. "cold") electrons thus produced was "heated" by (the very rapid) collisions with incoming fast injected electrons. The electron/electron energy exchange collision time in the ionizing plasma is of the order of 1-2 usec, so that the "cold" electrons are readily "heated" by collision with the incoming

injected electrons. The energy required to excite and energize the initially "cold" electrons resulting from the first "fast" electron ionization, is supplied by the incoming injected electron current, however, the total rate at which this can occur is limited by the input *power* of the injected beam. Thus the increasing density of initially-cold electrons will rise until a power balance is reached. Analysis of this process shows that injection currents of 10-40 A, at the injection energy of 12-12.5 kV, provides enough power to yield almost *complete* ionization of the neutral D gas (by this two-step – cold/hot –process) at a density of ca. 0.5-1E13/cm3, equivalent to a pressure (at STP) of about 3E-4 torr.

At these currents the complete ionization process takes place in less than 0.5 msec, by which time the electrons will nearly all be at the injection energy, because of the rapid 1-2 usec heating by electron/electron collisions during the process. With full ionization of the internal fill gas, the beta=one condition is reached (first with cold electrons) and maintained, as all the electrons are driven to injection energies by electron/electron collisions. The potential well is maintained, and the ions thus produced are able to make fusion reactions at or near the center of the well, by colliding with other ions at the bottom of the well

Data from the last one of these tests (10 November 2006) is shown in Figures 7 - 11

The measured data from these tests shows DD fusion neutron production (Fig. 7) of about 5E4 neutrons over a period of about 0.2 msec (less than the data rate interval), which also shows the emitter current of injected electrons (Fig. 8) to run at about 4-40 A during this short pulse period of fusion generation. .This peak pulse period is also indicated by light output measurements from the photomultiplier tube detectors (Fig. 9). The PMT showed a rise to peak output as the internal machine neutral gas was fully ionized, a flat-top during the onset of the external glow discharge, and a rapid falloff as this condition was passed. The actual rise was certainly faster than the data rate showed, so that at the peak, the edge electron density was a maximum, the full well depth was established, and DD fusion was taking place. Beyond this time, the potential on the machine dropped (Fig. 10) as external arcing (from the tank walls and feedthroughs) took over, the external current rose to very high values (Fig. 11), and the system discharged and shut down.

As the fill process proceeded, a lesser fraction of the neutral gas injection leaked out of the machine to the tank, however the tank pressure continued to rise. Since continued inflow of neutral gas from the pulsed supply could not be stopped in a fraction of a msec, gas flooded from the machine, both before and after the beta=one condition was reached.and filled the main vacuum tank within a few msec. This simply continued the tank wall arcing that started almost as soon as the well was formed, and the tank pressure continued to rise sufficiently so that the external arcing outside the machine system continued as well. This took place between the input leads carrying power to the device itself, and the tank walls and sharp corners surrounding these leads. These leads were not electrically shielded or insulated, so were able to arc with electrons from the large area of

surrounding tank metal. The Paschen arc condition here was dominated by the edges and corners of the tank wall reentrant structure at the feedthrough positions.

The current measuring devices used to measure emitter current all measured this current with respect to ground. The emitter current channel was independent of that used for the external current measurement (which showed the currents due to glow discharge and arcing). Thus the emitter current was correctly measured (Figure 8) as was the external "dumping" currents, recorded as rising to over 4000 A, as shown in the data traces of Figure 11, following the deep well production, beta=one condition.

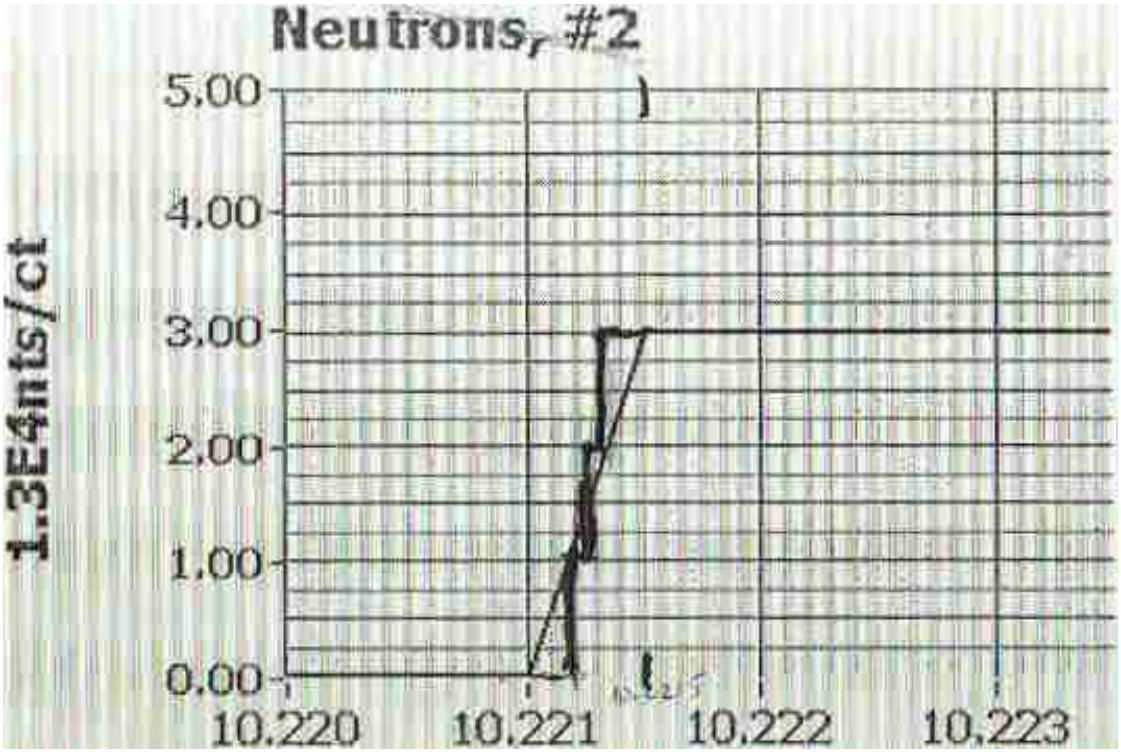

Figure 7. Neutron production in WB-6 pulse. Fusion rate is twice neutron rate

.

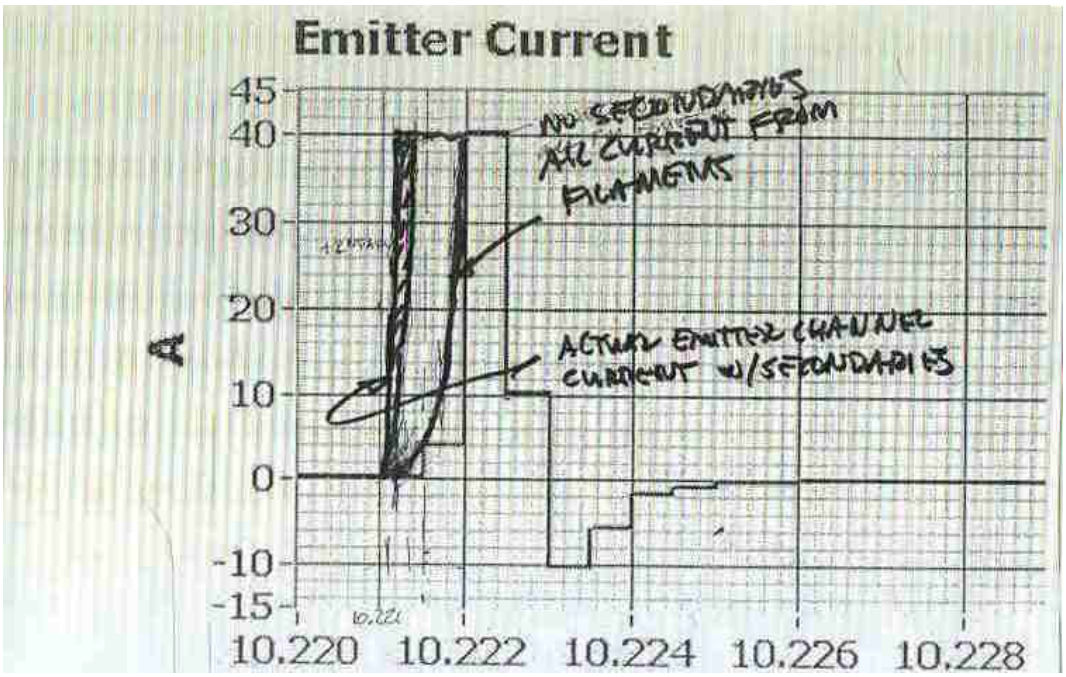

Figure 8. Emitter current during WB-6 short potential well pulse

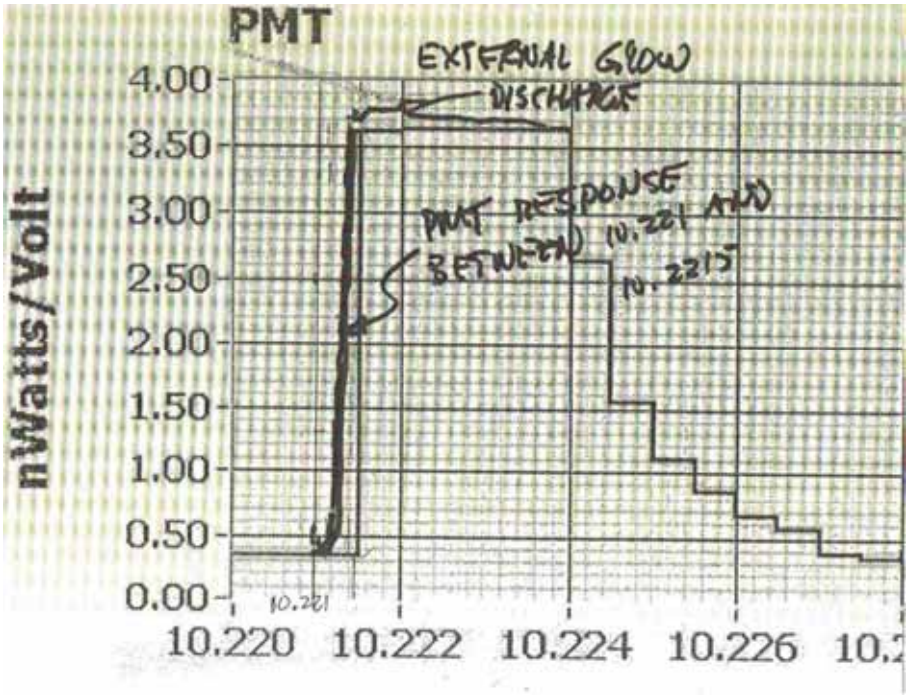

Figure 9. Photomultiplier tube output during short WB-6 pulse, and in after-glow discharge

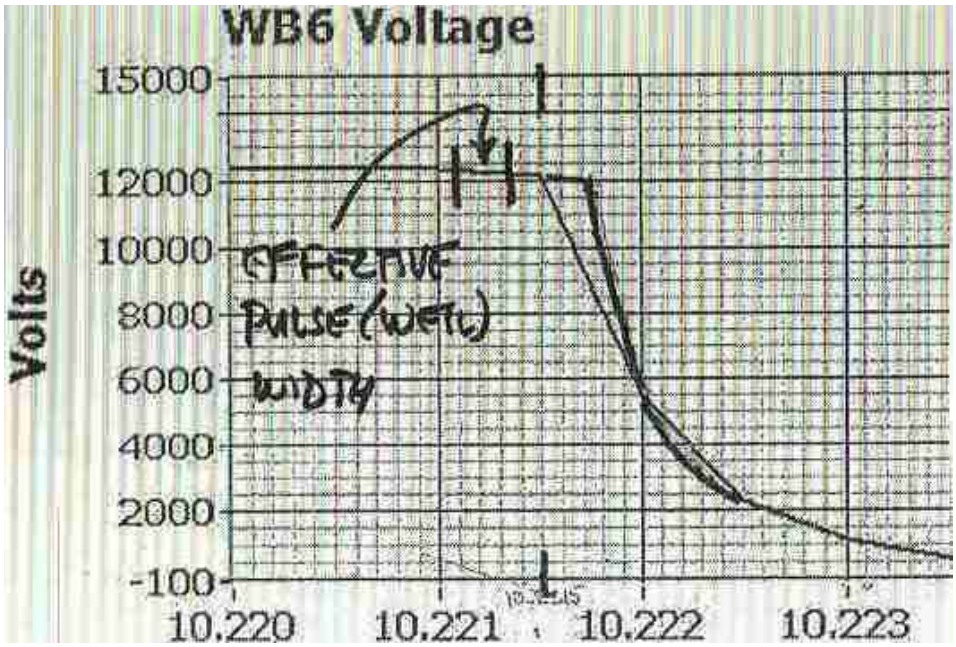

Figure 10. WB-6 voltage; note effective width of fusion pulse, and falloff with external arcing

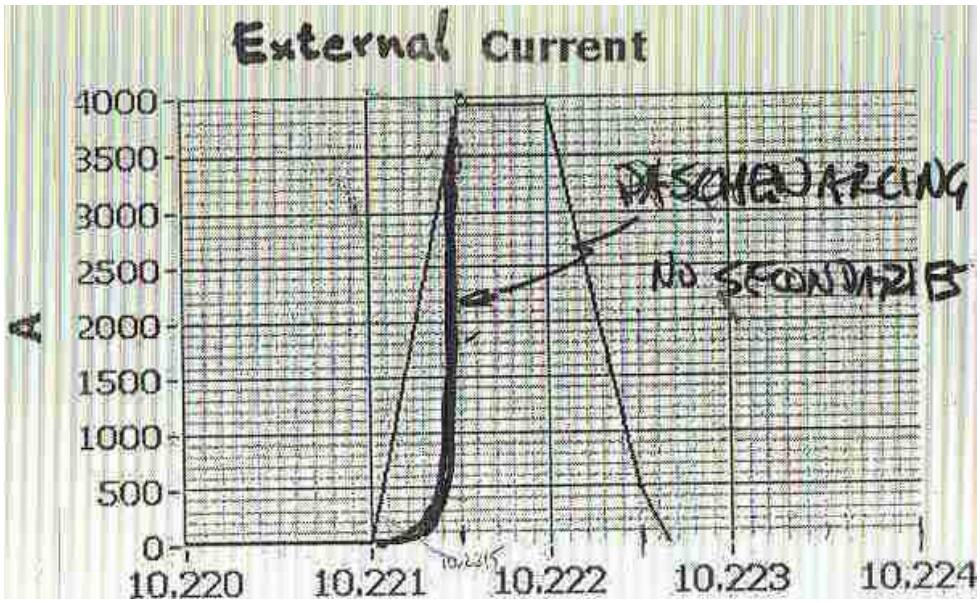

Figure 11. External current from feedthroughs to tank , cage, and WB-6 case

All tests had to be run in a completely transient mode, with puff gas input, emitter/extractor potentials supplied by pulsed electric drive from large capacitor banks, and with pulsed magnet currents, as well. This testing strategy was the only one possible in the laboratory setup and under the budgets available, as no power supplies were available to drive the system steady-state and the machine was much too small (by 10x) to allow design and construction of any steady-state cooling means for the magnet coils for such operation. In this method of testing, proper timing is the key to success of the tests.

The capacitor drive on the emitters/machine potentials was turned on first, by means of a fast-acting pneumatic-driven copper block switch, with the background gas pressure kept low, at ca,.1E-7 torr, to avoid arcing in the system. At this pressure, the emission was very small so that the caps did not discharge rapidly. Then the D gas was injected by a fast-acting (ca. 0.5-1 msec) solenoid valve, that opened the line from the gas chamber at 300 mtorr to the interior of the machine. The gas was stored in a small finite volume (ca. 8 cm3) of tubing, upstream of the machine. This caused the pressure and gas density to rise within the machine interior, with a rise time of about 0.3-0.5 msec. Fast injected electrons then ionized the gas as it reached its high density state, with consequent cascade ionization, as described above.

As this process proceeded, neutral gas unavoidably leaked out of the machine into the main vacuum tank, causing the pressure external to the machine to rise. Its leak rate was also on a time scale of about 0.3-0.5 msec. Since the tank volume was about 300 times larger than the volume of the WB-6 device, itself, the rise rate was correspondingly reduced. Initially the leaking gas filled the space between the machine and its Faraday cage, which was only about 6 times the machine volume. Thus glow discharge could take place in this region before the full tank was filled.

However, Paschen arcing will occur in the external regions of the system if the external pressure/density rises above about 3E-6 torr. Starting at 1E-7 torr, thus gives a rise factor of only about 30 for the avoidance of Paschen arcing in the entire external regions. Such arcing will – of course – shut the system down by causing a massive discharge of the capacitor bank into the arcs so formed. Since the pressure/density rise inside the machine must be from 1E-7 to 3E-4 torr equivalent, or about 3000x,while that allowed externally to avoid arcing is ca. 30x, the factor of 300 in external volume (above) allows about 3 msec to reach and hold internal test conditions desired for fusion in this test system. The initial glow discharge in the machine/cage space required far less time. And, as will be seen from the data obtained, these are reached in ca. 0.5 msec, beyond which the continued inflow of neutral gas does flood the tank and lead to external arcing, largely from tank power input leads to the tank walls themselves. The only solution to this problem is to utilize a very fast-acting shutoff valve in the feed line and/or to more carefully control the amount of gas available for feed by using a smaller feed reservoir volume, tailored to fit the minimal requirements of machine fill with little left over for external flooding. These methods will both be employed in the next small machine tests (WB-7,8).

Earlier Beta=One Tests

Before running at high drive voltages, it was useful to test for electron transport in this configuration. Since the key variable in such tests is the electron density at the machine inner edge, and since there was no way available to measure this density directly, it was noted that the density could be determined with precision if the machine could be run at the beta=one condition. This is evident from the formula for plasma electron beta: Beta = (8pi)(ne)(Ei)/B^2. If run at beta=one, with known drive voltage/energy Ei and known B field strength, the density will be uniquely determined. The beta=one condition can be measured by PMT data, which will always peak when the electron density reaches its maximum, which occurs only when this is achieved. Thus, if Ei is fixed, and the B field is swept from zero to a high value, it will always pass through the beta=one condition. At this point the density will be calculable, thus the electron transport coefficient in the MG transport equation can be determined for this point.

First tests, in October 2005, were made at low drive voltages with B fields sweeping from zero to several kG, to test for electron transport across the confining magnetic fields. By sweeping the B field of the machine, the range of plasma/electron "beta" was varied from infinity (at B = 0) to very small values (as B -> kG). In this sweep, it was inevitable that a value of B was reached at which plasma beta was equal to unity. At this condition, the electron density reached its maximum value, as this is the best that can be done by B fields to confine charged particles. This is easy to detect by use of light intensity measurements detecting electron/neutral ionization and subsequent recombination collision effects in the system. Accordingly, a photomultiplier tube (PMT) detector was used to measure light output as the B field was swept through its range. About 30 tests were made in this fashion.

Electron Losses to Surfaces

With the edge density thus determined, it is possible to calculate the coefficient (Kj) in the simplistic single-term electron cross-field transport equation, as derived from tests stretching from WB-2 through WB-4. This is

Ie = Kj(Ei)(SQRT(n))/B^(3/4)

where Ie is electron current in Amps, and other terms are as before. Results of these beta=one tests showed greatly improved confinement of electrons (by 10-20x) from prior work, and determined the overall transport coefficient in the simplistic one-term MaGrid transport equation to be much smaller than was found in earlier tests with prior machines.. This showed the efficacy of the WB-6 design in reducing electron losses in Polywell systems. These results also offered convincing proof that the actual transport of electrons across the B fields is only one component of the two-term loss channel mechanism discussed previously.

This mechanism involves both direct cross-field transport to the coil container surfaces (as cited above) , and losses to the less well-shielded surface areas at, for example, the coil/coil corner regions and/or to the edges of square coil boxes as used in earlier machines. In WB-2, 3 and 4 the coils touched at the corners, and this gave a direct loss area into the metal surface at these points, as the B fields went directly into the metal here. In WB-6 these corners were separated to avoid this problem, but less well-shielded interconnects still existed between coils, which offered higher loss flux regions than for the direct cross-field transport to the B-field-conformal coil containers. .

Losses to these less-well-shielded surfaces can be calculated (in the fashion of the enhancement of flow losses at the corners) as the product of the local density (nlocal) at the surface, the electron speed (ve), and the fractional area (funsh) of the lossy surfaces relative to the total loss area of the machine. The local density is given by the interior edge density (ne) reduced by the square root of the internal Gwb factor, to account for the interconnect position outside the magnetic field mid-plane. This gives an equation for such losses in WB-6, as

Iunsh = (funsh)(ne)(ve)/4{SQRT(Gwb)]((ks)

Where (ks) = 2(pi) E18 charges/sec per Coulomb, for Iunsh in Amps.

When the device is operating at beta = one, the inner edge density is just that from the pressure balance equation

(ne)(keEe) = (beta)(B^2)/8(pi)

where (ke) = 1.6E-12 ergs/eV, for Ee in eV, B in G, and ne in electrons/cm^3.

Taking these together, noting that Gwb = (BR)^2/110Ee in the truncated cube system, and reducing, gives the current Iunsh as

Iunsh = 1.05 (funsh)(B/R)

From this it is evident that the fraction of unshielded metal that can be tolerated for loss currents in the range of a few Amps, must be the order of funsh < 0.05 (5% of total surface area), or so.

Finally, because of the shortness of time and limited available effort, it was only possible to test WB-6 at conditions of interest for fusion for a few tests; four times at electron drive voltages (and consequent well depths) that might produce fusion. Drive energies were 12-12.5 keV, and well depths were at ca. 10 keV. These final tests all did produce measureable neutron counts, an indication of DD fusion, in a hopeful, yet rushed, ending to the program.

Figures 7 – 11, given previously, show data from one such test (on 10 November 2005), marked to indicate the current at which the well depths and densities were those desired for fusion, and at which fusion occurred. Note that the neutron counts were all obtained in a period less than 0.3 msec (the time scale of the data is on 0.5 msec intervals), and analysis shows that the fusion operating condition was only about 0.2 msec. For this operating period, the data show that the fusion rates produced in these tests were very large, typically at about 1E9 DD fusions/sec. This is over 100,000 times larger than results obtained in the much earlier work by Farnsworth/Hirsch at similar drive conditions Although these tests set a world's record for fusion output, the lack of funding from the USN required that the entire laboratory be shut down by 31 December 2005, and it was necessary to start the tear-down of the lab the Monday following these tests.

The following section of this report gives a summary review of the WB-6 experiments, including a brief review of the models that show the phenomenological behaviour patterns of the system. This is a more detailed description of the means employed in testing, and of the results obtained.

DISCUSSION OF THE EXPERIMENTS: SETUP, PROCEDURE AND RESULTS

Summary Model of Polywell Behaviour

The simple version of the Waffle Ball theory for fusion is as follows. WB (wiffle ball) machines are designed such that a quasi-spherical magnetic field is created, and electrons are injected into it. Once sufficient density of electrons is in the interior of the magnetic "ball", the high internal current density will push the interior field out, by electron current diamagnetic flow, so that the arrangement will resemble the child's toy, called a Wiffle Ball, with many "holes", or cusps. Only at these cusps will electrons be able to escape, while the other parts of the ball will very effectively contain the electrons, thus creating and confining a negative potential well in the center of the field. Losses to the non-cusp parts of the system are by electron transport, by collisions and instabilities, across the magnetic field to the coil containers. This is why the containers MUST be conformal to the fields the coils produce, and why NO metal surface must be intersected directly by field lines themselves.

The longer the electrons can be contained, and kept from reaching the case that houses the magnetic coils, the less current that must be continually injected to keep up with the losses, and the less power that is needed to drive the given machine. Thus, keeping magnetically insulated the surface to which electrons want to travel becomes very important. Two main potential configurations have been tried to achieve this. One is with the magnetic field windings (and/or their case) at high positive voltage, and the electron emitters at ground. The other has the electron emitters at high

negative potential, while the magnet windings are at ground. WB-6 employed the former, WB-5 was only focused on the latter, and WB-4 used both methods.

WB-4 had a large amount of magnetically unshielded metal, so that electron losses were inherently high and confinement time was small. WB-5 was supposed to solve that, but the closed box does not mimic the shape of the magnetic fields (if such can ever be done effectively). Therefore, it too had large unshielded sections (the seams and cusp end plates on the box), where electrons would escape into the metal of the box walls.. Without electron confinement for a minimal period of time, no fusion is possible without excessive drive currents..

Setup and Design

WB-6 was designed to be the remedy to WB-5, as it was for WB-4 before it. In truth, WB-6 is more like WB-4, in that it is an open-box, Wiffle-Ball machine that could be biased or left at ground potential. WB-5 was a closed-box system, in which only the emitters could be biased, leaving the vacuum tank walls at ground, much like the PXL experiments before it.

WB-6 was designed with six wound, toroidal magnets that would comprise the sides of the "box". Its design was a refinement of previous models, with uncooled magnets, meant only to be run for short durations (several seconds). Further, the magnets were designed with a round cross-section, unlike WB-4 with its square cross-section for the magnet winding case. This made the containing shells conformal to the shape of the magnetic fields, and thus avoided the deadly problem of fields intersecting metal surfaces directly.

WB-4 and 5 both had a problem with the seams of their box configurations. If one cuts the corners off a cube, one can see that the seams are what hold the sides together. Unfortunately, any electron following a field line will encounter one of these seams, should the magnetic field line go through it (and they do). Ideally, the magnets that form the six sides should sit close (adjacent) to one another, without actually touching. Even so, the box, itself, must then be shaped so as to be conformal to the overall field shape of the magnet system. Since this is a highly cusped geometry, it seems impossible to build such a box, and the whole idea of closed box systems appears to be wholly impractical.

In WB-6, each face magnet had to be fastened to its neighbors, and the finite thickness of metal structure led to a spacing of about one centimeter between each magnet, at the outside edge of the containing box. A small, cylindrical tube of metal was then welded at each "seam", so that each magnet had four such connecting pieces, connecting it to the adjacent round-cross-section coils. Some of these small cylinders housed current carrying wires, as well. These supports were inevitably an electron loss, but their location outside the mid-plane of the overall magnetic field kept these losses to a minimum, and the high field at the inter-coil spaces helped to keep the local density gradients high so the impact losses would be low.

The legs of the machine were hidden as well as possible inside tapered ceramic supports. While they could be "seen" electrostatically by electrons outside the machine interior, it was hoped that the ceramic insulators would keep the legs from becoming a major loss of electrons. Further, unlike WB-4, each leg would have current-carrying conductors running through it, so that there would be some degree of magnetic shielding.

The conductors then ran to a high-voltage feed-through, and then out to the magnetic field power supply (the main lab battery rack), and the high voltage bias power supply (12, 225uF capacitors, charged up to 15kV with the Hipotronics power supply). The path to the capacitor bank was broken by a large, copper, pneumatic switch, which could be closed at the operator's discretion, to apply high voltage to the already powered magnets.

The electron emitters were banks of headlight filaments, as these had proven inexpensive and durable in past tests. These filaments were run from car batteries, and activated by a fiber-optically isolated Siemens switch.

Gas was supplied by a small tube running from outside the tank, all the way to one of the coil/coil spaced seam areas. The last section of the gas supply tube was insulating material (glass), and the tube opening was just inside the surface of the box proscribed by the magnets. The gas supply was set up to be "puffed" in, as in previous tests. Gas input was controlled by a fast-acting (< 1 msec) solenoid valve separating the tank interior section from a small length of known volume (approximately 5 cm3), upstream, kept at known pressure. The line pressure was usually 300mtorr, while the vacuum tank pressure would start at the low 1E-7 torr range. The isolated, pressurized length of tube filled with D2 allowed starting with a known mass of gas, and thus allowed determination of the density inside the machine when the gas was injected.

The diagnostics available for these tests included 3 neutron counters (at varying distances), 2 black and white ccd cameras (not recording), one color camcorder (recording), a sensitive photomultiplier tube (PMT) system, and an optical spectrometer. Of course, all drive and power voltages and currents were measured and recorded, as well.

Procedure, Beta=1 tests

Several beta=1 tests were run during October, 2005, to try and determine the value of Kj, the MaGrid transport equation coefficient, which sets the loss rates for cross-field losses of electrons. This coefficient and the equation itself have been studied extensively over the preceding 7 years of experimental work, and are documented in several EMC2 Technical Reports. .

In this work the emitters were turned on, then the machine was biased using either the Hipo power supply or the Universal Voltronics, to 1500V, and 5000V. After this, the magnetic field drive

current was swept from zero up to 1000A (which gives an on-axis – face axis – field of about 1250-1300 G). As previously explained, at low field the magnetic beta is very large, much greater than unity, while – as the field sweeps up – the beta drops, until it becomes much less than unity. Hence, during the sweep, the field will pass through the point at which the electron beta is equal to unity. Since the beta=one condition is that at which the electron density is a maximum due to its optimal confinement, the PMT will show a peak in light output (from ionization collisions of trapped electrons with background neutral gas). This then allows accurate calculation of the electron density from the defining equation for beta; beta = nE/B^2.

Procedure, 12 Cap Bank Tests

The operating procedure was as follows:

1) Open the copper switch.
2) Ensure gas solenoid switch is closed. (tank pressure < 1E-6 torr)
3) Enable all recording instrumentation.
4) Charge section of gas tubing to desired value (usually 300mtorr).
5) Activate heating current for emitters, via Siemens switch.
6) Enable the Hipo power supply, and charge capacitors to desired voltage.
7) Disable Hipo, via "Stop Charge", while leaving caps charged.
8) Turn on magnetic field to desired value, via battery bank IGBTs.
9) Close copper switch, thus allowing emitters to start emitting electrons
10) Quickly close relay for gas solenoid, releasing gas into system, and discharging capacitor bank.
11) Turn off uncooled magnets, once sure caps have discharged.
12) Secure emitters, gas line, high voltage, and stop recording data.

The majority of the tests were run with three lab staff, which proved sufficient to to operate the system components remotely. With effort this could be done with two personnel, but more support is always preferable. .

Testing

The beta=one tests were illuminating, in that it was found that the PMT readings would maximize and then stay trelatively constant for a region after beta passed below and around unity. This is entirely consistent with the results of numerous particle-in-cell computer simulations and calculations made in past years, which show that the electron lifetime in cusp trapping systems rises with increasing current drive, peaks, and then decreases as beta=one is passed. The product of the drive current and the lifetime is a measure of the total electron density in the system, and this tends to reach a maximum at the beta=one condition, and then stay relatively flat for further increases in current (or corresponding increases in beta). The point at which the PMT readings show an inflection is then the best indication of achievement of beta=one.

From this work, the data showed that the MaGrid transport coefficient (in the simplistic one-term MG equation) was found to be about 10-20x less than from previous experiments on earlier machines. This is a logical result of the fact that the MG transport really involves two terms, one being the simple direct transport term and one being that due to unavoidable losses through seam-like line-cusp areas at the inter coil joint spaces, where the trapping factor may be very much less than that for the direct WB coil container surface regions. This has been discussed previously, in equations given above. The main result here is that, for WB-6, the simple single-term coefficient is Kj = 2-4E-12.

After running the beta = 1 tests, the experiments turned to higher voltages to test for fusion output. In this, it proved possible to run only five tests on WB6 before it self-destructed. The first was a test of the 12 capacitor bank used as the electron emitter drive power supply. This was used, as there were no power supplies available able to provide the currents needed to reach the beta=one conditions solely at high voltage drive, within anything resembling the budget limits of the program.
.

This large bank (twelve 225 uf capacitors, up to 15 kV) was proof tested under the shadow of the underdamped circuit that existed in the system (R^2C/4L < 1). This testing was done at 5 kV, to avoid over-driving the cap system at its first outing. Since the test time was very short, the underdamping proved not a problem, and work continued.

The next tests were all at higher voltage drive, starting at 10 kV, the third was at 12.5 kV and the fourth was at 12.5 kV. The well depth in these tests was typically about 0.8 of the drive voltage, due to spatial spread of the electron velocities at entry to the polyhedral coil system. Even at 5 kV some fusions took place, almost certainly from beam/beam reactions. At 12.5 kV the measured neutron output also showed that beam/beam reactions (as ions collided with neutrals in the well) were occurring. These tests were made on 9/10 November 2006. The neutron counts were in the range of 3 counts per test, for the closest counters, which calibrates out to about 5E5 fusions during the device operating time. Magnetic fields were in the range of 1000-1300 G. .

The final day of testing, 11 November 2006, was an attempt to run again at 12.5 kV, at 1300 G, but the device shorted and destroyed itself, while producing one count from fusions in the system. The caps were charged and, before firing, it was noted one of the input conductor support legs was sparking and glowing white hot, like a roman candle. Just then the caps were fired, which destroyed the arcing leg as they discharged.

Later inspection showed that the damage was due to local heating at the tight bend that was the junction for the leg. An internal short had occurred in the main power supply to the magnet windings, and these melted at the turning corner point on one leg. This, of course, ended the testing.

Summary of last 5 tests

1) 5.0kV, 800A B-field, 1 count
2) 9.8kV, 750A B-field, 2 counts
3) 12.5kV, 700A B-field, 2 counts
4) 12.5kV, 800A B-fiel (1 kG) d, 3 counts
5) 14kV, 1000A B-field, 1 count (while leg failing)

Notice that while the joint that eventually failed was glowing, according to the current sensor, there was still 1000A going through the magnet just before it was destroyed. And the last count recorded does occur at the time of the gas discharge, which occurred as the switch was closed. Also, the charging voltage was dropping just at the time the count occurs, and by the time it has registered, the voltage is still 10kV. The WB6 voltage divider is actually reading a negative number, and is clearly affected by the ongoing failure.

The last count (or perhaps any of the counts) is possibly able to be dismissed as noise. However, there are many reasons not to do so. First, the other 2 counters are close enough to pick up noise, but register nothing (we extensively shielded all 3 during WB5 testing). They are far enough, however, to not register the counts, the next closest one being double the closest distance, therefore at ¼ the flux. Maximum counts were 3, so even that would not show up on the further counters. Thus, the relative counts are consistent (unlike some of the older tests on WB4).

Second, during tests where the counters were unshielded, the max noise counts were during the closing of the copper switch. We don't see any counts during that.

Third, external stimuli were generated purposely to try to create noisy conditions on several earlier tests, but the counters failed to pick up any.

Fourth, the PMT registered a large pulse for 4 of the 5 tests, indicating a large light output, ***in the center of the machine***, at exactly the time of the counts. There is nothing there in the PMT's field of view to cause an arc (which usually is the culprit for noise).

Conclusion

Although more tests would have been desired, the runs that were made were very illuminating. The improvement in design greatly improved performance of the machine, since neutron counts were registered for all tests, something that did not occur for all of the tests with WB4. The flaws in WB6 are fairly obvious: lack of cooling, tight bends on the magnet wiring, very short duration tests, with limited ability to monitor what happens, lack of diagnostics, etc.

Despite these limitations, the results of the tests made show that the idea of fusion experiments using this model is a viable one, that should be pursued. Everything that was done could be improved, simply by adding funding. More people, better electron guns, better diagnostics, and better power supplies. Being able to run for even tens of milliseconds would help enormously in showing what exactly is occurring in the center of the quasi-spherical magnetic field of the device.. Unfortunately, this would never have been possible, even with added funding, in the then-existing lab location, due to power constraints of the building itself.

While these tests can not be construed to "prove" that *steady-state* fusion reactions can be produced and controlled in WB-6 like devices, or their larger cousins, nothing has been found or noted that would indicate a fatal flaw in such behaviour. Every test run has served to support the conviction that this type of inertial electrostatic confinement fusion has great potential, and is lacking only the resources for its full exploration and exploitation.